# *S*-wave resonances in positron-sodium scattering

Huili Han,[1,3] Zhenxiang Zhong,[1,3] Xianzhou Zhang,[2] and Tingyun Shi[1]
[1]*State Key Laboratory of Magnetic Resonance and Atomic and Molecular Physics, Wuhan Institute of Physics and Mathematics, Chinese Academy of Sciences, Wuhan 430071, People's Republic of China*
[2]*Department of Physics, Henan Normal University, XinXiang 453007, People's Republic of China*
[3]*Graduate School of the Chinese Academy of Sciences, Beijing 100049, People's Republic of China*
(Received 24 July 2007; published 29 January 2008)

We have calculated *S*-wave resonances in the positron-sodium system using the stabilization method in the framework of hyperspherical coordinates. Resonances below the Ps($n=2$) threshold have been investigated. We have located all the previously known *S*-wave resonances by Kar and Ho [Eur. Phys. J. D **35**, 453 (2005)] and Ward *et al.* [J. Phys. B **22**, 3763 (1989)] and observed relatively good agreement for the resonance positions. In addition, two new higher-lying resonances associated with the Ps($n=2$) threshold are found to be at energies of −0.066 56 and −0.063 53 a.u.

DOI: 10.1103/PhysRevA.77.012721 PACS number(s): 34.80.Uv, 31.15.xj, 33.40.+f

## I. INTRODUCTION

There has been continuous interest in the investigation of atomic resonances involving positrons [1–13], among which the positron-alkali-metal atom scattering has attracted considerable attention because of its unique opportunity for studying the positronium (Ps) formation [11–13]. The pioneering work on resonance phenomena in positron-alkali-metal systems has been performed by Ward *et al.* [11] using the close-coupling method with a model potential to describe the interaction between the active electron and the ionic core. However, no positronium formation channel has been included in their calculations. Recently, Kar and Ho [13] have studied the resonances in the $e^+$-Na system using the stabilization method with Hylleraas-type basis functions and obtained the resonances associated with the Na($3p$) and Na($4s$) thresholds. Although the resonance energies of Kar and Ho [13] are in reasonable agreement with those of Ward *et al.* [11], the resonance widths determined by these two groups are in disagreement. Up to now, only these two investigations on the resonance phenomena in the $e^+$-Na system have been reported. It should be noted that the resonances associated with the positronium thresholds have not been explored in a definitive way for the $e^+$-Na system. Although Kar and Ho [13] have found the higher-lying resonances converging to the Ps($n=2$) threshold through the stabilization plots, they have failed to extract the precise resonance parameters. The attractive interaction between the active electron and the positron leads to the formation of a positronium cluster in the outer valence region of the atom, resulting in the slow convergence for the binding energy. Thus an extraction of higher-lying resonances is not an easy task.

In this paper, we will focus on searching for *S*-wave resonances in the scattering of a positron from the atomic sodium using the stabilization method in the framework of hyperspherical coordinates. The hyperspherical method has been successfully applied to resonance calculations by several authors [3–5,14]. However, these calculations have been based on the scattering approach for the determination of resonance parameters. The stabilization method, on the other hand, is one of the simplest and powerful tools for studying resonances, which needs only the diagonalization of a real matrix with the varying box size $L$ to obtain the stabilization diagram. The flat plateau in the vicinities of avoided crossings corresponds to the occurrence of a resonance for a particular system concerned. The physical origin of the flat plateau is that a resonance scattering wave function is localized at short range, and as such, the resonance energy is stabilized. By calculating the density of resonance states in the vicinity of the avoided crossing, one can obtain the resonance energy $E_r$ and the resonance width $\Gamma$ [12,15]. The hyperspherical potential curves, on the other hand, provide a useful means for locating the resonance positions and for understanding why they are formed [3,14].

Recently, we developed a computational scheme to calculate the binding energies and geometrical properties for the $e^+$-Na and the $e^+$-Li systems using the hyperspherical method [18]. Our results are in good agreement with the best calculations using the fixed-core stochastic-variational method (FCSVM) [19]. In the present study, we will use the same method to solve the energy eigenvalue equation for different box size. By adjusting the knot distribution of *B*-splines to characterize the behavior of channel functions, a great improvement over the convergence of potential curves can be achieved. Therefore highly accurate potential curves and channel functions can be obtained, which is essential for extracting higher-lying resonances.

## II. THEORY

We treat the $e^+$-Na system as a three-body one which consists of a core, an electron, and a positron. The core is assumed to have infinite mass. We use $r_e$, $r_p$, and $r_{ep}$ to represent the electron-core distance, the positron-core distance, and the electron-positron distance, respectively. The angle between $r_e$ and $r_p$ is denoted by $\theta$. The hyper-radius $R$ and the hyperangle $\phi$ are defined by

$$R = \sqrt{r_e^2 + r_p^2} \tag{1}$$

and

 

$$\tan\phi = \frac{r_p}{r_e}, \tag{2}$$

respectively. Atomic units are used throughout unless otherwise stated. Since we consider states with $J=0$ only, the Schrödinger equation then involves only the three internal coordinates $R$, $\phi$, and $\theta$. We first rescale the original wave function $\Psi$ according to [16]

$$\psi(R,\phi,\theta) = \Psi(R,\phi,\theta)R^{3/2}\sin\phi\cos\phi. \tag{3}$$

Then the Schrödinger equation can be recasted into

$$\left(-\frac{1}{2}\frac{\partial}{\partial R}R^2\frac{\partial}{\partial R} + H_{ad}(R,\phi,\theta)\right)\psi(R,\phi,\theta) = R^2E\psi(R,\phi,\theta), \tag{4}$$

where $H_{ad}$ is the adiabatic Hamiltonian

$$H_{ad}(R,\phi,\theta) = \frac{\Lambda^2 - \frac{1}{4}}{2} + R^2V(R,\phi,\theta) \tag{5}$$

with

$$\Lambda^2 = -\frac{\partial^2}{\partial\phi^2} - \frac{1}{\sin^2\phi\cos^2\phi\sin\theta}\frac{\partial}{\partial\theta}\left(\sin\theta\frac{\partial}{\partial\theta}\right) \tag{6}$$

and $V(R,\phi,\theta)$ is the interaction among the three particles. The adiabatic potentials and channel functions are defined as the solutions of the adiabatic eigenvalue equation:

$$H_{ad}(R,\phi,\theta)\Phi_\nu(R,\phi,\theta) = U_\nu(R)\Phi_\nu(R,\phi,\theta). \tag{7}$$

The channel functions can be expanded in terms of $B$-splines as follows:

$$\Phi_\nu(R,\phi,\theta) = \sum_i^{N_\phi}\sum_j^{N_\theta} c_{i,j}^\nu B_i(\phi)B_j(\theta), \tag{8}$$

where $N_\phi$ and $N_\theta$ are the sizes of basis sets in the $\phi$ and $\theta$ directions, respectively. At this stage, the accurate potential curves and channel functions can be obtained by building up the behavior of channel functions explicitly into the knot distribution of $B$-splines. The details can be found in [17,18]. Equation (4) can be solved using the slow variable discretization (SVD) method. We only present the formulas that are used in the current work. The detailed description of the SVD method can be found in [20]. The solution $\psi(R,\phi,\theta)$ of Eq. (4) is expanded in terms of pointwise DVR (discrete variable representation) basis functions $\pi_j(R)$ which are constructed from Laguerre polynomials $L_n^\alpha(R/\beta)$ with $\alpha=3$ and the scaling factor $\beta=L/R_N$, where $R_N$ is the $N$th zero of $L_N^\alpha(R)$ and $L$ is the size of the system:

$$\psi(R,\phi,\theta) = \sum_{j=1}^{N_{\rm DVR}}\sum_{\mu=1}^{N_\mu} c_{j\mu}\pi_j(R)\Phi_\mu(R_j,\phi,\theta) \tag{9}$$

with $N_{\rm DVR}$ being the number of terms in the DVR basis set and $N_\mu$ the number of coupled channels. We rewrite the hyper-radial Schrödinger equation, Eq. (4), in the form of

$$\sum_{j=1}^{N_{\rm DVR}}\sum_{\mu=1}^{N_\mu}(K_{ij} - E\rho_{ij})O_{i\nu,j\mu}c_{j\mu} + U_\nu(R_i)c_{i\nu} = 0, \tag{10}$$

where

$$K_{ij} = \int_0^\infty \pi_i(R)\left(-\frac{1}{2\mu}\frac{\partial}{\partial R}R^2\frac{\partial}{\partial R}\right)\pi_j(R)dR,$$

$$\rho_{ij} = \int_0^\infty \pi_i(R)\pi_j(R)R^2dR, \tag{11}$$

and

$$O_{i\nu,j\mu} = \langle\Phi_\nu(R_i,\phi,\theta)|\Phi_\mu(R_j,\phi,\theta)\rangle \tag{12}$$

is the overlap matrix element between two adiabatic channels defined at different Gauss-Laguerre quadrature points.

To extract the resonance energy $E_r$ and the resonance width $\Gamma$, we first plot the stabilization diagram versus the varying box size $L$ and then calculate the density of resonance states for two energy levels at the avoided crossing with the help of the following formula [15]:

$$\rho_n(E) = \left|\frac{E_n(L_{i+1}) - E_n(L_{i-1})}{L_{i+1} - L_{i-1}}\right|^{-1}_{E_n(L_i)=E_i}, \tag{13}$$

where the index $i$ indicates the $i$th value of $L$. After calculating the density of resonance states $\rho_n(E)$ with the above formula, we fit it to the following Lorentzian form that involves the resonance energy $E_r$ and the width $\Gamma$:

$$\rho_n(E) = y_0 + \frac{A}{\pi}\frac{\Gamma/2}{(E-E_r)^2 + (\Gamma/2)^2}, \tag{14}$$

where $y_0$ is the baseline offset, $A$ is the total area under the curve from the base line, $E_r$ is the center of the peak, and $\Gamma$ is the full width of the peak of the curve at half height.

## III. RESULTS AND DISCUSSION

In order to test the validity of our approach, we first calculate the $S$-wave resonances below the Ps($n=2$) threshold in the $Ps^-$ system and then compare with other more elaborated calculations [10,14,21–25].

### A. $Ps^-$ results

For the $Ps^-$ system, we use the Jacobi coordinates which are different from the hyperspherical coordinates that will be used for the $e^+$-Na system. The hyper-radius $R$ is defined by $R^2=\frac{1}{2}\rho_1^2+\frac{3}{2}\rho_2^2$, where $\rho_1$ is the distance between the two electrons and $\rho_2$ is the distance between the center of the two electrons and the positron. We have computed the energy eigenvalues for 541 different $L$ values within the range of $L=101-155$ a.u., in intervals of 0.1 a.u. The basis-set parameters used are $N_\theta=30$, $N_\phi=50$, $N_{\rm DVR}=50$, and $N_\mu=20$, keeping the hyperspherical potential curves to have at least seven significant digits for the lowest 30 curves. The calculated ground state energy for this system is −0.262 005 01 a.u. with $L=100$ a.u., in comparison with

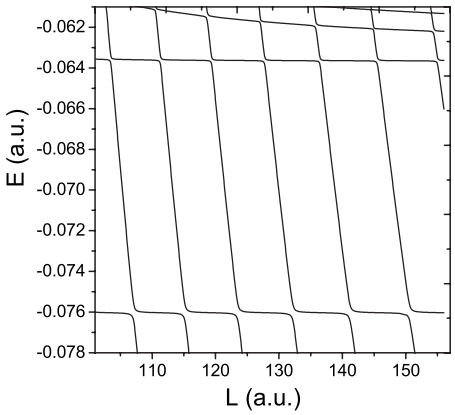


FIG. 1. Stabilization plot $E$ versus $L$ for the $S$ wave in $Ps^-$, in atomic units.

the more accurate variational result of Frolov [26] −0.262 005 070 232 980 107 770 375 a.u.

The stabilization diagram in Fig. 1 clearly shows the stabilization character near the energy $E_r=-0.076$ and −0.063 a.u., respectively, which are believed to be associated with the Ps($n=2$) threshold energy of −0.0625 a.u. Figures 2(a) show the density of resonance states $\rho_n(E)$ with varying energy eigenvalue $E$ for the lowest resonance below the Ps($n=2$) threshold. The solid circles are the results of actual calculations for $\rho_n(E)$ and the solid line is the fitted Lorentzian form. The resonance energies are thus determined to be $E_r=-0.076\,030\,3$ and $-0.063\,643\,1$ a.u. with the corresponding resonance widths of $\Gamma=0.000\,043\,0$ and 0.000 011 3 a.u., respectively.

Table I lists a comparison of our results for the $S$-wave resonances in $Ps^-$ below the $n=2$ threshold with other more elaborated calculations. Our calculations are in good agreement with the results of Ho [21], as well as with the results of Li and Shakeshaft [24], which are obtained by the method of complex-coordinate rotation, except for the width of $2s3s$ where the value of Li and Shakeshaft is smaller than the values of Ho and ours. Similar comparison can be made with the results of Zhou and Lin [14] using the close-coupling method in hyperspherical coordinates. In summary, we have successfully applied our method to the $Ps^-$ system for both bound and resonance states. Let us now shift our attention to the $e^+$-Na system.

### B. $e^+$-Na results

For the $e^+$-Na system, the interaction among the three charged particles is given by

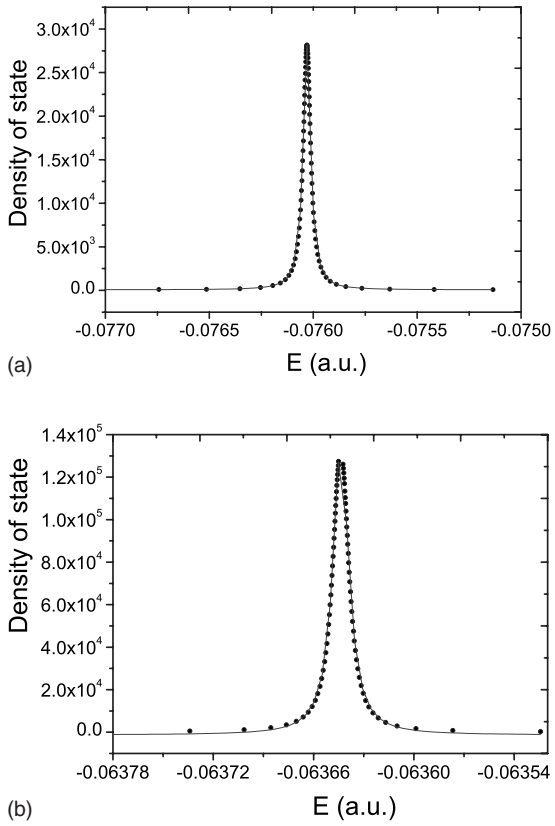


FIG. 2. The fitting of the density of resonance states (solid circles) to the Lorentzian form for the $S$ wave in $Ps^-$. The full curve is the fitting. (a) The resonance parameters are determined to be $E_r=-0.076\,030\,3$ a.u. and $\Gamma=0.000\,043\,0$ a.u. (b) The resonance parameters are determined to be $E_r=-0.063\,643\,1$ a.u. and $\Gamma=0.000\,011\,3$ a.u.

$$V(R,\phi,\theta)=V_-(r_e)+V_+(r_p)+V(r_{ep}), \tag{15}$$

where $V_-(r_e)$ is the model potential describing the interaction between the valence electron and the core, $V_+(r_p)$ is the model potential between the position and the core, and $V(r_{ep})$ is the model potential between the electron and positron. The model potential for the valence electron and the core has the form

$$V_-(r)=-\frac{1}{r}[Z_c+(Z-Z_c)e^{-a_1 r}+a_2 r e^{-a_3 r}]-\frac{a_c}{2r^4}\left[W_3\left(\frac{r}{r_c}\right)\right]^2, \tag{16}$$

where

TABLE I. Comparison of the $S$-wave resonance $E_r$ and width $\Gamma$ below the $n=2$ threshold for the $Ps^-$ system with other calculations, in atomic units.

| | Present work | Ho [21] | Li and Shakeshaft [24] | Papp *et al.* [6] | Zhou and Lin [14] | Toyota and Watanabe [23] |
|---|---|---|---|---|---|---|
| $2s2s$ | $E_r=-0.0760303$<br>$10^5\Gamma=4.30$ | $E_r=-0.07603040$<br>$10^5\Gamma=4.3$ | $E_r=-0.07603044$<br>$10^5\Gamma=4.30345$ | $E_r=-0.07595$<br>$10^5\Gamma=4.25$ | $E_r=-0.07604$<br>$10^5\Gamma=4.35$ | $E_r=-0.076029875$<br>$10^5\Gamma=4.3094461$ |
| $2s3s$ | $E_r=-0.0636431$<br>$10^5\Gamma=1.13$ | $E_r=-0.06365$<br>$10^5\Gamma=1.0$ | $E_r=-0.06364918$<br>$10^5\Gamma=0.867850$ | $E_r=-0.06365$<br>$10^5\Gamma=0.85$ | $E_r=-0.063675$<br>$10^5\Gamma=0.875$ | $E_r=-0.0636482263$<br>$10^5\Gamma=0.873396269$ |

TABLE II. Comparison of the calculated bound state energies of Na with the experiment values, in atomic units.

| | Na | | |
|---|---|---|---|
| State | Present | Experiment [29] | Kar and Ho [13] |
| $3s$ | −0.188855 | −0.18886 | −0.18886 |
| $3p$ | −0.111538 | −0.11154 | −0.11152 |
| $4s$ | −0.071581 | −0.07158 | −0.07158 |
| $3d$ | −0.055941 | −0.05594 | |
| $4p$ | −0.050939 | −0.05094 | −0.05102 |

$$W_n(r) = 1 - e^{-r^n} \tag{17}$$

is the cutoff function used to assure the correct behavior at the origin. The second term in Eq. (16) describes the polarization of the core, where $a_c = 0.9457$ is the $Na^+$ polarizability [27]. Also in Eq. (16), the nuclear charge is $Z=11$ and the charge of the $Na^+$ core is $Z_c=1$. The remaining parameters, which are $a_1 = 3.324\,424\,52$, $a_2 = 0.713\,727\,98$, $a_3 = 1.832\,818\,15$, and $r_c = 0.524\,506\,38$, are fitted by [28] using the least-squares method to reproduce the experimentally measured energy levels of the Na atom.

Using the model potential given in Eq. (16), we have calculated the energies of the ground and excited states of Na by diagonalizing the Hamiltonian using $B$-splines as basis sets. The calculated energies are nicely comparable with the experimental results, as shown in Table II. In the table we also contain the results of Kar and Ho [13] who used a similar model potential without the core polarization term. Our results agree with the experimental values, as well as with the values of Kar and Ho [13].

For the positron-core potential $V_+(r_p)$, the sign of the static potential in Eq. (16) is changed but the polarization term remains the same. The rationality of such an approximation has been discussed in [13,30]. Previous calculations [13,18,30] indicate that the inclusion of the exchangelike potential would not introduce a significant error into the final results. Finally, the electron-positron interaction is given by

$$V(r_{ep}) = -\frac{1}{|\vec{r}_p - \vec{r}_e|} + \frac{\alpha_d}{r_e^2 r_p^2} \cos\theta\, W_3\left(\frac{r_p}{r_c}\right) W_3\left(\frac{r_e}{r_c}\right), \tag{18}$$

where the second term is analogous to the dielectronic correction which ensures that there is no core polarization when the positron and electron coalesce.

For the $e^+$-Na system, efforts have been made in optimizing the knot distribution of $B$-splines to overcome the problem of slow convergence of the binding energy $\varepsilon$ and the satisfying results have been obtained [18]. Table III is the comparison of our calculations for $e^+$-Na with the other available results. The values in column three are obtained by the FCSVM method with the core polarization term included in the model potential; and the values in column four are without the core polarization term. In our calculation, since the polarization term has been included in the model potential, our results are close to the results of [19]. The value in column five is given by Le *et al.* [32] who used the hyperspherical method but with much larger sizes of basis sets.

Since the binding energy is more rapidly converged than the expectation values, smaller basis sets are usually enough in calculating resonances. We have computed the energy eigenvalues for 841 different $L$ values within the range of $L = 80-101$ a.u., in intervals of 0.025 a.u. The parameters used are $N_\theta = 20$, $N_\phi = 63$, $N_{\mathrm{DVR}} = 65$, and $N_\mu = 30$, keeping the hyperspherical potentials to have at least six significant digits for the lowest 30 curves. The calculated ground state energy is converged to −0.250 443 a.u. using these parameters. Figure 3(a) shows the stabilization character near the energy $E_r = -0.1105$ a.u. Figure 3(b) shows the stabilization character near the energies $E_r = -0.076$ −0.070, −0.066, and −0.063 a.u., respectively. These resonances lie below the Ps($n=2$) threshold −0.0625 a.u. Figure 4 shows the density of resonance states $\rho_n(E)$ for the lowest resonance. From the figure, we have located a shape resonance just above the Na($3p$) threshold of −0.111 538 a.u. A fit to the formula of Eq. (14) has yielded the resonance position of $E_r = -0.110\,833\,0$ a.u. and the width of $\Gamma = 0.000\,041$ a.u. The reason for its formation can be understood by examining the hyperspherical potential curves.

In the adiabatic hyperspherical approach, the Schrödinger equation for the system can be written as [16]

$$\left[-\frac{1}{2}\frac{d^2}{dR^2} + \frac{U_\mu(R)}{R^2} + W_{\mu\mu}(R) - E\right] F_\mu(R) = 0, \tag{19}$$

where

$$W_{\mu\mu}(R) = -\frac{1}{2}\left\langle \Phi_\mu(R,\theta,\phi) \left| \frac{d^2}{dR^2} \right| \Phi_\mu(R,\theta,\phi) \right\rangle \tag{20}$$

is the diagonal coupling term. It can be shown [33,34] that the ground state energy obtained by solving Eq. (19) is an

TABLE III. Energies and various expectation values (in atomic units) for $e^+$-Na. The parameters used are $L=250$, $N_\phi=123$, $N_\theta=20$, $N_{\mathrm{DVR}}=70$, and $N_\mu=20$.

| | $e^+$Na | | | |
|---|---|---|---|---|
| Quantity | Present | FCSVM with polarization [19] | FCSVM without polarization [31] | Hyperspherical [32] |
| $E$ | −0.250447 | −0.250473 | −0.250177 | |
| $\varepsilon$ | 0.000447 | 0.000473 | 0.000177 | 0.000453 |
| $\langle r_e \rangle$ | 17.12 | 16.818 | 23.73 | |
| $\langle r_p \rangle$ | 17.52 | 17.231 | 24.00 | |
| $\langle r_{ep} \rangle$ | 3.159 | 3.162 | 3.09 | |

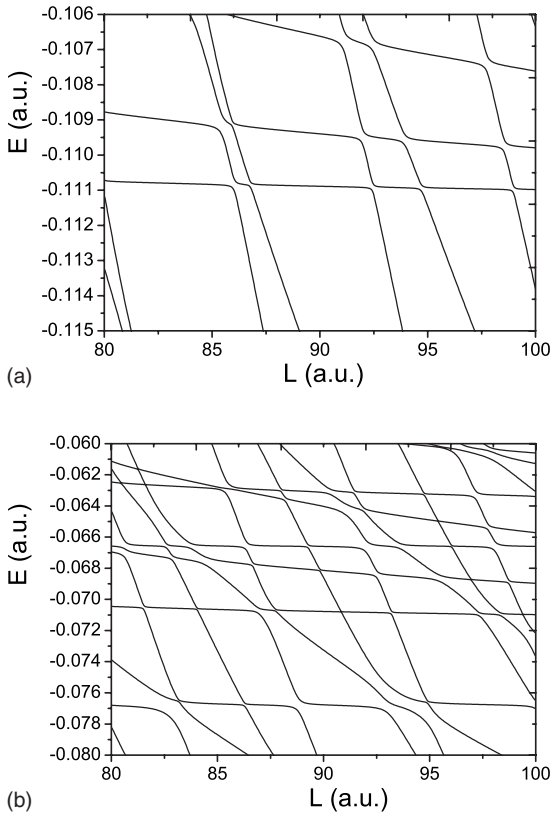


FIG. 3. Stabilization plot $E$ versus $L$ for the $S$ wave in $e^+$-Na, in atomic units.

upper bound to the true ground state energy. If we solve Eq. (19) without $W_{\mu\mu}(R)$, the ground state energy obtained in this way is a lower bound to the ground state energy. Equation (19) is similar to the single-particle radial Schrödinger equation with the potential $V_\mu(R)=[U_\mu(R)/R^2]+W_{\mu\mu}(R)$. The positron-sodium scattering is thereby reduced to the potential scattering problem with the potential $V_\mu(R)$ for each channel $\mu$, and the properties of bound states or scattering states for each channel $\mu$ are related directly to the shape of the potential $V_\mu(R)$.

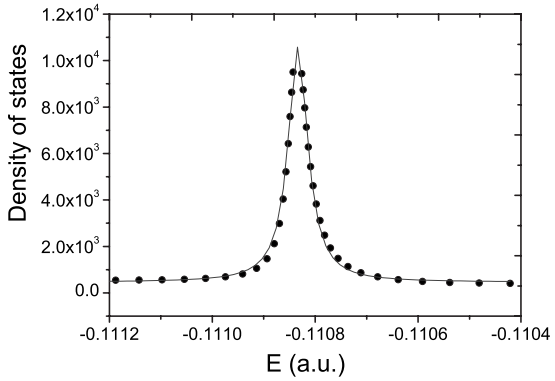


FIG. 4. The fitting of the density of resonance states (solid circles) to the Lorentzian form for the $S$-wave $e^+$-Na system. The full curve is the fitting. The resonance parameters are determined to be $E_r=-0.110\,833\,0$ a.u. and $\Gamma=0.000\,041$ a.u.

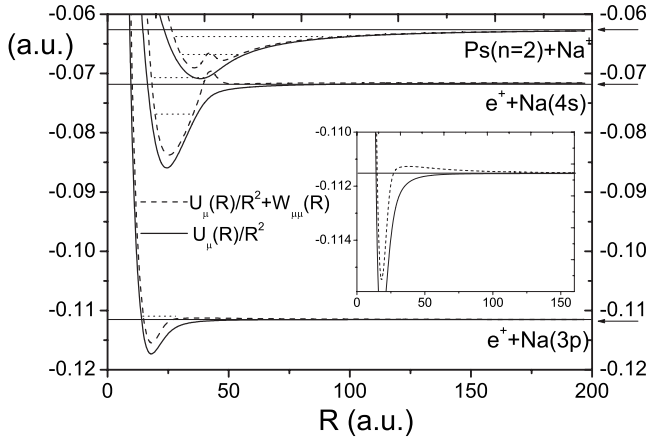


FIG. 5. The hyperspherical potential curves $V_\mu(R)=\frac{U_\mu(R)}{R^2}+W_{\mu\mu}(R)$ (dashed line) and $\frac{U_\mu(R)}{R^2}$ (solid line) for the $e^+$-Na system are shown as functions of the hyperspherical radius. These are the only curves which support resonances in our calculation. The solid horizontal lines indicate the different thresholds and the dotted lines represent the resonance positions. The inset is the magnification of a part of the lowest curve.

The calculated $S$-wave hyperspherical potential curves $V_\mu(R)$ for the $e^+$-Na system are shown in Fig. 5. The solid horizontal lines indicate the different dissociation thresholds and the dotted lines are the positions of the resonances. The potential curve $V_\mu(R)$ converging to the Na($3p$) threshold has a potential barrier which supports the shape resonance as seen in Fig. 5.

Figure 6 shows the density of resonance states $\rho_n(E)$ for the second and third resonances, respectively. The fitting of Fig. 6(a) gives rise to a Feshbach resonance below the Na($4s$) threshold with the resonance position of $E_r=-0.076\,801\,0$ a.u. and the width of $\Gamma=0.000\,140$ a.u. Similarly, the fitting of Fig. 6(b) gives rise to a shape resonance just above the Na($4s$) threshold with the resonance position of $E_r=-0.070\,940\,1$ a.u. and the width of $\Gamma=0.000\,047$ a.u. To analyze the origin of these resonances, it is useful to examine the hyperspherical potential curves $V_\mu(R)$ near this energy region in Fig. 5. These two resonances are related to the potential curve $V_\mu(R)$ converging to the Na($4s$) threshold $-0.071\,581$ a.u., which has an attractive well at small $R$ and a potential barrier at large $R$. More importantly, Fig. 5 indicates that the lowest curve from the Na($4s$) and the Ps($n=2$)+$Na^+$ threshold interacts with each other strongly, showing a pronounced avoided crossing at $R\approx 40$ a.u. Such an avoided crossing may modify the spectral behavior of those obtained using a single isolated potential curve. For example, the resonance without considering the coupling would yield the energy $E=-0.0762$ a.u.

Figure 7 is the density of resonance states $\rho_n(E)$ for the fourth and fifth resonances, respectively, which are believed to be associated with the Ps($n=2$) threshold. Figure 7(a) shows the resonance parameter of $E_r=-0.066\,560\,6$ a.u. and $\Gamma=0.000\,061$ a.u. Figure 7(b) shows the resonance parameters of $E_r=-0.063\,530\,1$ a.u. and $\Gamma=0.000\,041$ a.u.

It should be mentioned that the last two resonances associated with the Ps($n=2$) threshold were not obtained by the

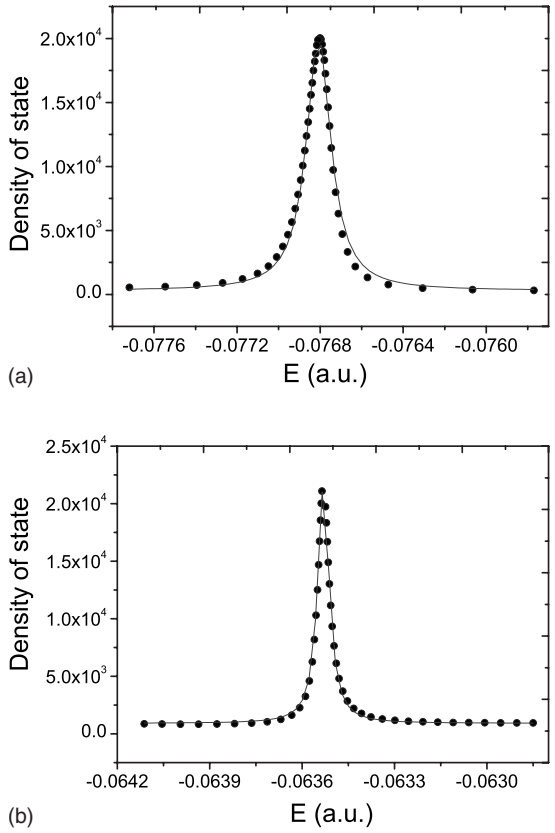


FIG. 6. The fitting of the density of resonance states (solid circles) to the Lorentzian form for the *S*-wave $e^+$-Na system. The full curve is the fitting. (a) The resonance parameters are $E_r$= −0.076 801 0 a.u. and Γ=0.000 140 a.u. (b) The resonance parameters are $E_r$=−0.070 940 1 a.u. and Γ=0.000 047 a.u.

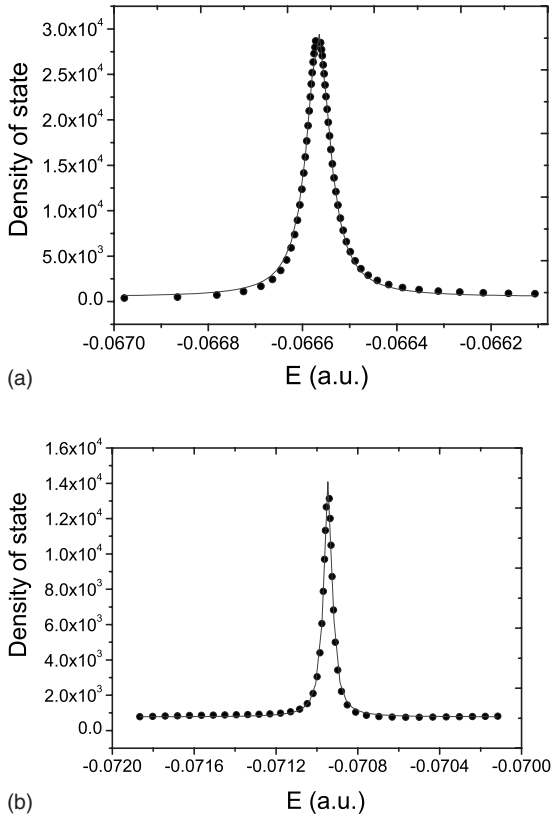


FIG. 7. The fitting of the density of resonance states (solid circles) to the Lorentzian form for the *S*-wave $e^+$-Na system. The full curve is the fitting. (a) The resonance parameters are determined to be $E_r$=−0.066 560 6 a.u. and Γ=0.000 061 a.u. (b) The resonance parameters are $E_r$=−0.063 530 1 a.u. and Γ =0.000 041 a.u.

previous two calculations [11,13]. We may give a convincing argument that the resonances indeed occur near the Ps($n$ =2) threshold by examining the hyperspherical potentials in Fig. 5. One of the potential curves converging to the Ps($n$ =2) threshold has an asymptotic attractive dipole potential due to the degenerate Ps($n$=2) states. This adiabatic potential curve supports an infinite series of bound states just below the Ps($n$=2) threshold. The two lowest of which are found to be located at −0.0675 and −0.0639 a.u. by solving Eq. (19) without the coupling term $W_{\mu\mu}(R)$. They shift slightly into −0.0658 and −0.0634 a.u., respectively, after the coupling term $W_{\mu\mu}(R)$ is included. These bound states turn into Feshbach resonances when coupled with open channels. Therefore we believe that these two higher-lying resonances indeed exist.

The convergence studies of the resonance parameters $E_r$ and Γ have been done by using different sizes of basis sets as shown in Table IV. One can see that the results are quite

TABLE IV. Convergence study of the resonance energy $E_r$ and width Γ for the $e^+$-Na system below the Ps($n$=2) threshold, in atomic units.

| | $s(1)$ | $s(2)$ | $s(3)$ | $s(4)$ | $s(5)$ |
|---|---|---|---|---|---|
| $N_\phi$=63, $N_\theta$=20 | $E_r$=−0.1108334 | $E_r$=−0.0768072 | $E_r$=−0.0709459 | $E_r$=−0.0665665 | $E_r$=−0.0635305 |
| $N_{\rm DVR}$=60, $N_\mu$=20 | Γ=0.000046 | Γ=0.000143 | Γ=0.000048 | Γ=0.000059 | Γ=0.000045 |
| $N_\phi$=83, $N_\theta$=20 | $E_r$=−0.1108336 | $E_r$=−0.0768072 | $E_r$=−0.0709467 | $E_r$=−0.0665666 | $E_r$=−0.0635305 |
| $N_{\rm DVR}$=60, $N_\mu$=20 | Γ=0.000046 | Γ=0.000142 | Γ=0.000048 | Γ=0.000059 | Γ=0.000045 |
| $N_\phi$=83, $N_\theta$=30 | $E_r$=−0.1108336 | $E_r$=−0.0768102 | $E_r$=−0.0709467 | $E_r$=−0.0665666 | $E_r$=−0.0635305 |
| $N_{\rm DVR}$=60, $N_\mu$=30 | Γ=0.000046 | Γ=0.000142 | Γ=0.000048 | Γ=0.000059 | Γ=0.000045 |
| $N_\phi$=83, $N_\theta$=30 | $E_r$=−0.1108330 | $E_r$=−0.0768010 | $E_r$=−0.0709401 | $E_r$=−0.0665606 | $E_r$=−0.0635301 |
| $N_{\rm DVR}$=65, $N_\mu$=30 | Γ=0.000041 | Γ=0.000140 | Γ=0.000047 | Γ=0.000061 | Γ=0.000041 |

TABLE V. Comparison of the *S*-wave resonance $E_r$ and width $\Gamma$ in the $e^+$-Na system with other calculations. The quoted values for $E_r$ are relative to the ground state energy of Na($3s$) in eV. The units for $\Gamma$ are meV.

| | Present | Kar and Ho [13] | Ward *et al.* [11] |
|---|---|---|---|
| $s(1)$ | $E_r$=2.12201 | $E_r$=2.219 | $E_r$=1.985 |
| | $\Gamma$=1.25 | $\Gamma$=5.58 | $\Gamma$=0.4 |
| $s(2)$ | $E_r$=3.04749 | $E_r$=3.076 | $E_r$=3.19 |
| | $\Gamma$=3.86 | $\Gamma$=11.7 | $\Gamma$=0.2 |
| $s(3)$ | $E_r$=3.20715 | $E_r$=3.346 | $E_r$=3.62 |
| | $\Gamma$=1.30 | $\Gamma$=8.44 | $\Gamma$=4 |
| $s(4)$ | $E_r$=3.32629 | | |
| | $\Gamma$=1.60 | | |
| $s(5)$ | $E_r$=3.40870 | | |
| | $\Gamma$=1.27 | | |

stable as the sizes of basis sets increase. The resonance position $E_r$ and width $\Gamma$ are converged to at least $10^{-5}$. Table V presents a comparison of our results with other theoretical calculations. The lowest three resonances have also been obtained by Kar and Ho [13], as well as by Ward *et al.* [11]. Our results for the resonance energy $E_r$ are in reasonable agreement with theirs. However, our values for the resonance widths differ considerably from that of Ward *et al.* [11] and Kar and Ho [13], which in turn also disagree with each other. We should mention that the positronium channels were not included in the Ward *et al.* work [11]. The discrepancies in width with Ward *et al.* may be due to the omission of the positronium channel in their calculations. There are also large discrepancies between our widths and those given by Kar and Ho [13], which is presumably due to the use of different model potentials in their calculations. More importantly, the core polarization term was not included in their model potentials. It has been demonstrated that the core polarization plays an important role in positron-alkali-metal systems. The work by Ward and Shertzer [35] for the $e^+$-Li system shows that the inclusion of the core polarization term in the model potential results in an increase in the positronium formation cross section. As for the $e^+$-Na system, changes in the core polarization potential can lead to greater changes in the binding energy and expectation values [18,36] as seen in Table III.

For the last two higher-lying resonances, no other theoretical and experimental investigations have been reported. Although Kar and Ho [13] have observed higher-lying resonances converging to the Ps($n$=2) threshold using stabilization plots, they have failed to extract the resonance parameters. The present method combined with more converged basis sets has enabled us to determine the positions and widths for the two higher-lying resonances. We believe that our results are reasonably accurate, as the convergence for the resonance parameters $E_r$ and $\Gamma$ is very well and the model potential between the electron and the core is capable of producing energy levels which nearly match the experimental values.

## IV. CONCLUSION

The stabilization method in hyperspherical coordinates has been used for the first time to study resonance. In order to check the validity of the method, we have first investigated the *S*-wave resonances below the Ps($n$=2) threshold in the $Ps^-$ system. The good agreement of our results with other calculations has indicated that our method may be capable of producing accurate results of resonance parameters for some atomic systems involving positron.

Using this method, we have also performed the calculations of *S*-wave resonances in the $e^+$-Na system below the Ps($n$=2) threshold. The five resonances located at −0.110 833 0, −0.076 801 0, −0.070 940 1, −0.066 560 6, and −0.063 530 1 a.u. have been determined, together with the corresponding resonance widths shown in Table IV. With the help of the adiabatic potential curves, we have also analyzed the nature of resonances. Our results have been compared with other calculations available in the literature.

## ACKNOWLEDGMENTS

This work was supported by the National Natural Science Foundation of China under Grants No. 10374119 and No. 10674154. The authors thank Dr. Z.-C. Yan for reading the manuscript and for clarifying the earlier unclear presentation.

[1] A. K. Bhatia and R. J. Drachman, Phys. Rev. A **42**, 5117 (1990).
[2] Y. K. Ho, Phys. Rev. A **53**, 3165 (1996).
[3] A. Igarashi and I. Shimamura, Phys. Rev. A **56**, 4733 (1997).
[4] K. Aiba, A. Igarashi, and I. Shimamura, J. Phys. B **40**, F9 (2007).
[5] D. I. Abramov and V. V. Gusev, J. Phys. B **38**, 4281 (2005).
[6] Z. Papp, J. Darai, C.-Y. Hu, Z. T. Hlousek, B. Kónya, and S. L. Yakovlev, Phys. Rev. A **65**, 032725 (2002).
[7] Z.-C. Yan and Y. K. Ho, J. Phys. B **36**, 4417 (2003).
[8] A. Igarashi and I. Shimamura, Phys. Rev. A **70**, 012706 (2004).
[9] N. Yamanaka, Y. Kino, and A. Ichimura, Phys. Rev. A **70**, 062701 (2004).
[10] A. Basu and A. S. Ghosh, Phys. Rev. A **72**, 062507 (2005).
[11] S. J. Ward, M. Horbatsch, R. P. McEachran, and A. D. Stauffer, J. Phys. B **22**, 3763 (1989).
[12] U. Roy and Y. K. Ho, J. Phys. B **35**, 2149 (2002).
[13] S. Kar and Y. K. Ho, Eur. Phys. J. D **35**, 453 (2005).
[14] Y. Zhou and C. D. Lin, Phys. Rev. Lett. **75**, 2296 (1995).
[15] V. A. Mandelshtam, T. R. Ravuri, and H. S. Taylor, Phys. Rev. Lett. **70**, 1932 (1993).
[16] C. D. Lin, Phys. Rep. **257**, 1 (1995).
[17] Hui-Li Han, Yong Li, Xian-Zhou Zhang, and Ting-Yun Shi, J.

Chem. Phys. **127**, 154104 (2007).
[18] Hui-Li Han, Xian-Zhou Zhang, and Ting-Yun Shi (unpublished).
[19] G. G. Ryzhik, J. Mitroy, and K. Varga, J. Phys. B **31**, 3965 (1998).
[20] O. I. Tolstikhin, S. Watanabe, and M. Matsuzawa, J. Phys. B **29**, L389 (1996).
[21] Y. K. Ho, Phys. Lett. **102A**, 348 (1984).
[22] J. Zs. Mezei and Z. Papp, Phys. Rev. A **73**, 030701(R) (2006).
[23] K. Toyota and S. Watanabe, Phys. Rev. A **68**, 062504 (2003).
[24] T. Li and R. Shakeshaft, Phys. Rev. A **71**, 052505 (2005).
[25] Z. Papp, J. Darai, J. Zs. Mezei, Z. T. Hlousek, and C.-Y. Hu, Phys. Rev. Lett. **94**, 143201 (2005).
[26] A. M. Frolov, Phys. Rev. E **74**, 027702 (2006).
[27] W. R. Johnson, D. Kolb, and K.-N. Huang, At. Data Nucl. Data Tables **28**, 333 (1982).
[28] C.-N. Liu and A. F. Starace, Phys. Rev. A **59**, 3643 (1999).
[29] G. York, R. Sheps, and A. Gallagher, J. Chem. Phys. **63**, 1052 (1975).
[30] J. Shertzer and S. J. Ward, Phys. Rev. A **73**, 022504 (2006).
[31] G. G. Ryzhik, J. Mitroy, and K. Varga, J. Phys. B **31**, L265 (1998).
[32] A.-T. Le, M. W. J. Bromley, and C. D. Lin, Phys. Rev. A **71**, 032713 (2005).
[33] A. F. Starace and G. L. Webster, Phys. Rev. A **19**, 1629 (1979).
[34] Y. Li, Q. D. Gou, and T. Y. Shi, Phys. Rev. A **74**, 032502 (2006).
[35] S. J. Ward and J. Shertzer, Nucl. Instrum. Methods Phys. Res. B **221**, 206 (2004).
[36] J. Mitroy, M. W. J. Bromley, and G. G. Ryzhik, J. Phys. B **35**, R81 (2002).